

This is the accepted manuscript made available via CHORUS. The article has been published as:

^{57}Fe Mössbauer spectroscopy studies of CaFe_4As_3

I. Nowik, I. Felner, A. B. Karki, and R. Jin

Phys. Rev. B **84**, 212402 — Published 7 December 2011

DOI: [10.1103/PhysRevB.84.212402](https://doi.org/10.1103/PhysRevB.84.212402)

^{57}Fe Mössbauer Spectroscopy Studies of CaFe_4As_3

I. Nowik and I. Felner

Racah Institute of Physics, The Hebrew University, Jerusalem, 91904, Israel

A. B. Karki, R. Jin

Department of Physics & Astronomy, Louisiana State University, Baton Rouge, LA 70803

We report the ^{57}Fe Mössbauer spectroscopy and dc magnetization studies of orthorhombic CaFe_4As_3 , which undergoes two magnetic transitions with the formation of spin density wave at $T_{\text{N1}} = 88$ K (incommensurate) and $T_{\text{N2}} = 26$ K (commensurate). The magnetic Mössbauer spectroscopy spectra below T_{N1} are composed of four sub-spectra attributed to the four in-equivalent Fe crystallographic sites: three Fe ions are in the divalent state (Fe^{2+}) and one as Fe^{1+} . However, the magnetic lines are much broader than that below T_{N2} , indicating an incommensurate magnetic state. In the paramagnetic state, the Mössbauer spectroscopy spectra are composed of three doublets, one of them is related to Fe^{1+} . Evidence for spin fluctuations above T_{N1} is observed.

PACS numbers 74.62.Bf, 74.70.Xa, 75.50.Ee, 76.80.+y

Introduction

Recently, much attention has been focused on the research of Fe-based materials, because they reveal superconductivity with transition temperature comparable to cuprates. The building block of these materials is either Fe-As or Fe-Se layer formed by edge-shared FeAs_4 or FeSe_4 tetrahedra. Prior to chemical doping or application of pressure in so-called parent compounds, these Fe-As or Fe-Se layers exhibit long-range three-dimensional antiferromagnetic (AFM) spin-density-wave (SDW) order at $T_{\text{N}} \sim 140 - 150$ K or $520 - 550$ K with Fe^{2+} moment of $0.87(3) \mu_{\text{B}}/\text{Fe}$ or $3.31 \mu_{\text{B}}/\text{Fe}$, respectively [1-2]. In BaFe_2As_2 the Fe moments are aligned within the ab plane [1], whereas neutron powder diffraction (NPD) shows that they are along the c axis in KFe_2Se_2 [2]. The major difference between the two systems, noticeable from several types of measurements, is that the temperature-composition phase diagrams show a generic behavior as a function of the substituent concentration (x) in the Fe-As based materials. This implies a systematic *suppression* of the magnetic transition by increasing x or pressure. Then, above a critical concentration (which depends on the substituent), superconductivity is observed [3-4]. On the other hand, the non-stoichiometric $\text{A}_z\text{Fe}_{2-y}\text{Se}_2$ also becomes superconducting around $30 - 33$ K, but the AFM state persists even at low temperatures [5-6]. This means, in $\text{A}_z\text{Fe}_{2-y}\text{Se}_2$, there is a *coexistence* of magnetism and superconductivity, since both states are confined to the same

Fe-Se crystallographic layer [5]. This makes the extensive search for new Fe-As based compounds inseparable from the search of new high - T_c superconducting materials.

The new compound CaFe_4As_3 is a good reference, as it has the same building block as Fe-As based superconducting compounds, i.e., edge – shared FeAs_4 tetrahedron. CaFe_4As_3 crystallizes in the orthorhombic structure (space group $Pnma$) with $a = 11.873 \text{ \AA}$, $b = 3.740 \text{ \AA}$ and $c = 1.574 \text{ \AA}$ [7], as reported in Ref. [8] and illustrated in Figure 1. NPD studies show that there are four independent Fe sites in the crystallographic unit cell, all of multiplicity four and in the $(x, 1/4, z)$ positions as reported in Ref. [8]. Electrical resistivity, magnetic susceptibility and specific heat studies reveal the existence of two transitions [9-11]. Below $T_{N1} \sim 88 \text{ K}$ an incommensurate SDW along the b axis is observed, which undergoes below $T_{N2} \sim 26 \text{ K}$ to a commensurate SDW state in the ac plane [8].

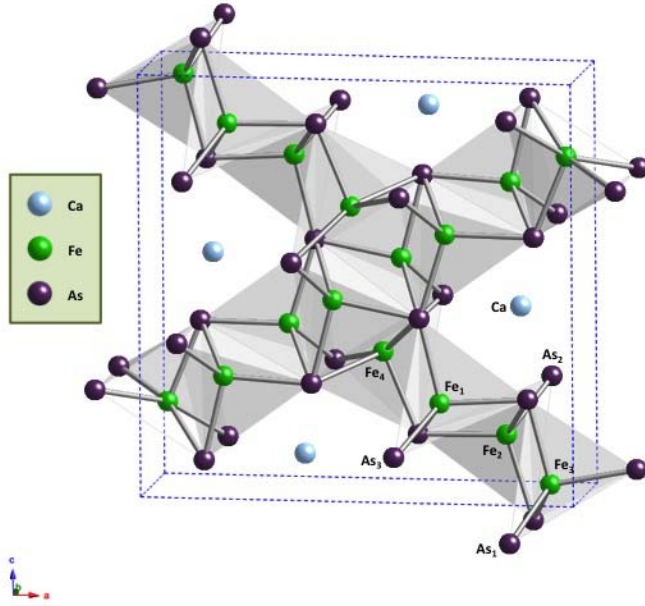


Figure 1: Crystallographic structure of CaFe_4As_3 with indication of four Fe sites.

Mössbauer spectroscopy (MS) of ^{57}Fe isotope seems particularly useful for studying CaFe_4As_3 system, as Fe makes the basic constituent of this compound. Formal charges of the various Fe ions can be assigned by assuming a complete electron transfer from the Ca and Fe cations to the As anions. In order to naturalize the unit cell charge, the formal Fe valences are three Fe^{2+} and one Fe^{1+} for Ca^{2+} and As^{3-} . Indeed, the room temperature (RT) MS study exhibits approximately two paramagnetic quadrupole subspectra with isomer-shifts (IS) of 0.32 (1) and 0.54(1) mm/sec and an intensity ratio of 3:1, thus confirming the

presence of the two Fe states [6]. Moreover, the substitution of Cr for Fe measured by NPD and MS show selectively Cr occupation in the Fe₄ site, which is attributed to the Fe¹⁺ site [12].

Our focus in this report is the comprehensive ⁵⁷Fe MS studies of CaFe₄As₃ in both commensurate and incommensurate magnetic states as well as in the paramagnetic (PM) region. In the PM region, the MS spectra are actually composed of three subspectra (intensities 2:1:1) and that are attributed to three Fe²⁺ and one Fe¹⁺ as identified by their isomer shifts (IS). Below T_{N1}, the MS are composed of four sub-spectra associated with the four in-equivalent Fe sites. In the commensurate region, the lines of all sub-spectra are much sharper than that in the incommensurate region.

Experimental details

Single crystals of CaFe₄As₃ were grown out of Sn flux. The detailed procedure is described in [9]. These crystals were ground into powder for measurements reported here. Zero-field-cooled (ZFC) temperature dependence of the magnetization measured under various applied fields was performed in a commercial MPMS5 Quantum Design SQUID magnetometer. Prior to recording ZFC curve, the SQUID magnetometer was adjusted to be in "real" H = 0 state. The ⁵⁷Fe Mössbauer studies of powder CaFe₄As₃ at temperatures 5 to 297 K, were performed using a conventional constant acceleration drive in transmission mode, in conjunction with a 50 mCi ⁵⁷Co:Rh source. The absorber was cooled to low temperatures in a Janis model SHI-850-5 closed cycle refrigerator. The spectra were analyzed in terms of least square fit procedures to theoretical expected spectra. The velocity-calibration was done by the spectrum of an α -iron foil. The reported IS are relative to this foil.

Experimental Results

Figure 2 shows the temperature dependence of magnetization (M) measured in the zero-field-cooled (ZFC) mode at 15 Oe for CaFe₄As₃ powder. The complicated temperature dependence of M is similar to that reported in Ref. [7]. The pronounced peak at T_{N2} = 26 K, the bent at T_{N1} = 88 K and a broad plateau at 88-112 K are readily observed. The isothermal field dependence of the magnetization M(H) measured at 5 and 140 K are presented in the inset. Both M(H) curves are not linear at low H. The linear part at 5 K reflects the AFM nature of the sample and the slope obtained is ~ 0.0135 emu/mole Oe. In the paramagnetic

range, the slope is ~ 0.0101 emu/mole Oe. The extrapolated values to $H = 0$ are 0.23 and 0.13 emu/g for $T = 5$ and 140 K, respectively. This means that a small fraction of a ferromagnetic extra phase is present, probably 0.06-0.1% of Fe, not detectable by x-ray diffraction and/or by MS. Above ~ 350 K, the compound follows the Curie-Weiss law [9].

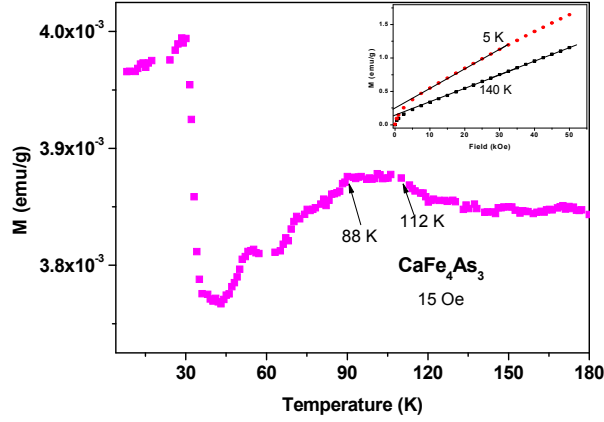


Figure 2: Temperature dependence of magnetization of CaFe_4As_3 powder measured at 15 Oe in ZFC mode. The isothermal magnetization at 5 and 140 K are shown in the inset.

^{57}Fe MS studies of CaFe_4As_3 at a wide range of temperatures have been performed. Figure 3 shows the MS of CaFe_4As_3 below (left panel) and above (right panel) T_{N1} . The hyperfine parameters deduced are summarized in Tables I – II. Due to the higher resolution in our spectra in comparison to those reported in Refs. [7, 12], we are confident that in the paramagnetic range (at 125 K and at room temperature), the spectra display *three* pure quadrupole spectra with a common line width of 0.263 mm/s and intensity ratio 2:1:1 (see Fig. 3). It seems that two of the Fe^{2+} sites are indistinguishable and have almost the same hyperfine parameters. The first two subspectra have similar IS (0.32 mm/s and 0.33 mm/s at 297 K) corresponding to Fe^{2+} , but possess different quadrupole interactions $\text{EQ} (=1/4e^2qQ)$ (see Table I). The hyperfine parameters of the third subspectrum are much larger: IS = 0.535 mm/s, and $\text{EQ} = 0.248$ mm/s, which may correspond to Fe^{1+} [6]. The larger IS values at 125 K, relative to that obtained at 297 K, is due to the thermal shift as expected.

| T (K) | | 2Fe^{2+} | Fe^{2+} | Fe^{1+} |
|-------|-------------|-------------------|------------------|------------------|
| 125 | I.S. (mm/s) | 0.45(1) | 0.45(1) | 0.67(1) |
| | EQ (mm/s) | 0.10(1) | 0.20(1) | 0.26(1) |

| | | | | |
|-----|-------------|---------|---------|---------|
| 297 | I.S. (mm/s) | 0.32(1) | 0.33(1) | 0.53(1) |
| | EQ (mm/s) | 0.10(1) | 0.17(1) | 0.25(1) |

Table I: Isomer shift (IS) and quadrupole splitting (EQ) of CaFe_4As_3 in the paramagnetic state.

As can be seen in Fig. 3, the spectra display four equally intense subspectra (fixed intensity ratios) below T_{N1} , revealing additional magnetic splitting with distributions in hyperfine fields (H_{eff}) which is typical to spin density wave Mössbauer spectra. All subspectra were fitted with a fixed common line width of 0.284 mm/s. While the resolution of the separate absorption lines is reasonable at 5 K (below T_{N2} , the commensurate SDW region), the spectra become much worse at $T_{N2} < T < T_{N1}$ (the incommensurate SDW region), even though they display little change in total width. The observed four H_{eff} values

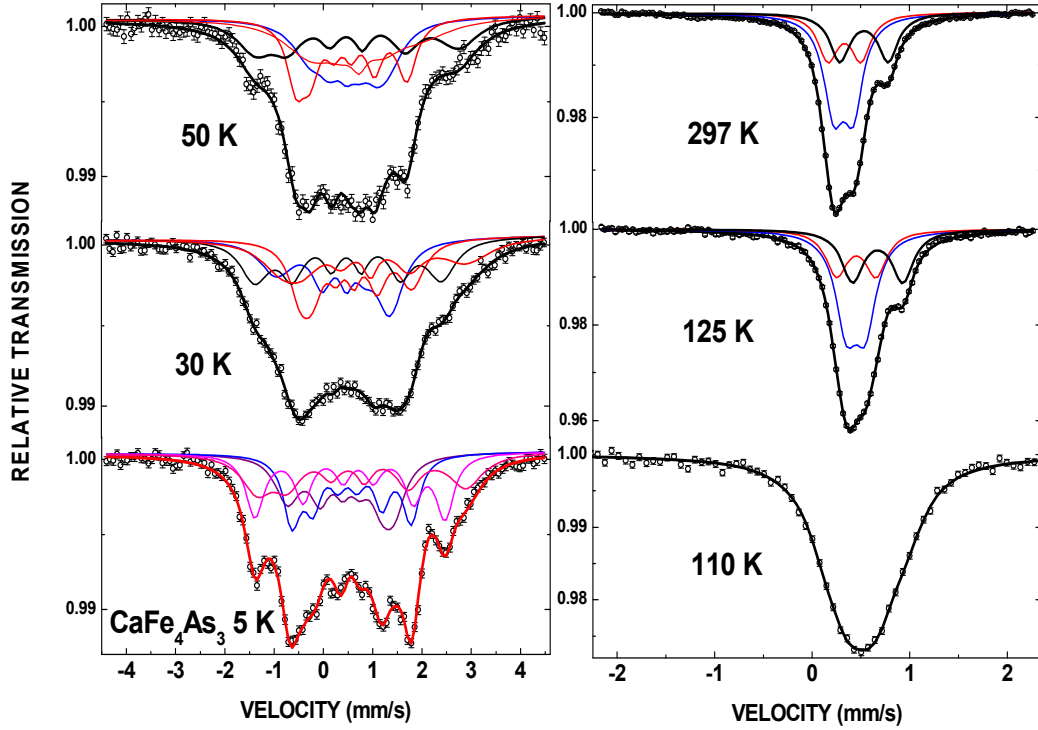


Figure 3: Mössbauer spectra of CaFe_4As_3 below (left) and above (right) $T_{N1} = 88$ K. Notice the different scales.

in Table II, are due to four inequivalent Fe sites. At 5 K, the largest IS = 0.805 mm/s (in comparison with the others with IS less than 0.547 mm/s) is attributed to Fe_4 (Fe^{1+}),

following the assignment done in Refs. [8,12]. The higher IS values at 5 K relative to that obtained at room temperature, is due (as expected) to the second-order Doppler Effect. From the H_{eff} values obtained at 5 K one may deduce the saturated magnetic moment (M_S) acting on the Fe ions at low temperatures. In general, H_{eff} is proportional to the magnetic moment M_S . Therefore, the H_{eff} values obtained are attributed to M_S of the four sites deduced from NPD [8]. The constant of proportionality, $\beta = H_{\text{eff}}/M_S$, is $\sim 6 \text{ T}/\mu_B$ in the present case. This value is much smaller than that obtained for Fe or Fe_2O_3 ($\sim 11\text{-}15 \text{ T}/\mu_B$) and is consistent with the conclusion made in Ref. [13]. According to Ref. [13], β depends on various parameters, thus the scaling of H_{eff} and M_S is not unique. The spectrum obtained at 50 K is quite similar to that of 30 K (see Fig. 3). As it is in the incommensurate SDW state, the hyperfine values deduced at 50 K are not conclusive and therefore are not included in Table II. It is worth mentioning that magnetic spin fluctuations exist above $T_{\text{N1}} = 88 \text{ K}$. Fig. 3 shows a broad spectrum at 110 K, compared to the spectra at 125 K and room temperature. This is consistent with the broad maximum observed in magnetization (see Fig. 2).

| T (K) | | Fe ₁ | Fe ₂ | Fe ₃ | Fe ₄ (Fe ¹⁺) |
|-----------|-------------------------------------|-----------------|-----------------|-----------------|-------------------------------------|
| 5 | IS (mm/s) ± 0.01 | 0.50 | 0.55 | 0.37 | 0.81 |
| | EQ_{eff} (mm/s) ± 0.01 | 0.03 | 0.08 | -0.24 | 0.13 |
| | H_{eff} (T) ± 0.2 | 11.6 | 7.2 | 7.5 | 11.5 |
| | M_S (μ_B) at 1.5 K | 2.14 | 1.55 | 1.83 | 1.94 |
| 30 | IS (mm/s) ± 0.01 | 0.48 | 0.55 | 0.43 | 0.84 |
| | EQ_{eff} (mm/s) ± 0.01 | 0.01 | 0.11 | -0.20 | 0.18 |
| | H_{eff} (T) ± 0.2 | 11.7 | 7.0 | 7.2 | 11.6 |
| | M_S (μ_B) at 30 K | 1.40 | 1.61 | 1.67 | 1.84 |

Table II: Isomer shift (IS), effective quadrupole interactions ($EQ_{\text{eff}} = EQ \cdot \frac{1}{2}(3\cos^2(\Theta) - 1)$ (where Θ is the angle between the hyperfine field and the axis of the local electric field gradient responsible for the quadrupole interaction), magnetic hyperfine field (H_{eff}) of CaFe_4As_3 in the magnetic states, and the magnetic moment amplitudes M_S obtained from NPD studies [8].

As far as the MS studies are concerned, we may compare the magnetic properties of CaFe_4As_3 to the two related SDW BaFe_2As_2 and KFe_2Se_2 compounds, in which the Fe ions reside in one crystallographic site only. The various shapes of the SDW state for the BaFe_2As_2 system are discussed in details in Ref. [14]. BaFe_2As_2 is magnetically ordered at $T_N = 136(1) \text{ K}$, with Fe^{2+} moments of $0.87(3) \mu_B/\text{Fe}$ aligned within the basal plane [1]. Below T_N , all our MS spectra of BaFe_2As_2 were analyzed in terms of a superposition of

commensurate and incommensurate SDW subspectra with an average H_{eff} (5.53 ± 0.6 T at 5 K) [15]. Thus $\beta = 6.3$ T/ μ_B was obtained, and is very similar to that of CaFe_4As_3 . On the other hand, KFe_2Se_2 is AFM ordered up to ~ 520 K, with Fe^{2+} moments of $3.31 \mu_B/\text{Fe}$, which forms a collinear AFM structure along the c axis [2]. Our MS studies show clearly that $H_{\text{eff}} = 28.1$ T at 93 K. In contrast to Ref. [2], the best fit to the experimental data is obtained only when the Fe moments are tilted by $\theta \sim 44^\circ$ from the c axis [16]. For KFe_2Se_2 , the ratio $\beta = 8.5$ T/ μ_B . Again, this proves that the scaling of H_{eff} and M_S is not unique as proposed in Ref. [13].

Another point of interest is the high IS obtained (0.81 mm/s at 5K) for one sub-spectrum of CaFe_4As_3 , which is attributed to Fe^{1+} (Fe_4 site). Such a state is seldom observed. As stated above, one Fe ion must be in a lower formal valence while the rest three Fe ions are in the divalent state in order to preserve neutrality of CaFe_4As_3 . High spin Fe^{1+} is not found in stable compounds, but its existence has been shown as a substitutional impurity in good insulator ionic lattices, as transients after radio-active decay as observed for ^{57}Co decay in TiO_2 [17], MgO or CaO or when $^{57}\text{CoCl}_2$ is doped into KCl [18-19]. The fact that the stable Fe^{1+} state is observed in a compact *metallic* system is unique and deserves more studies. Further experimental and theoretical work is needed to establish its entire physical and chemical properties.

In summary, the four in-equivalent Fe ions in CaFe_4As_3 undergo two magnetic transitions: (1) an incommensurate spin density wave order of the Fe ions below $T_{N1} = 88$ K and (2) a commensurate AFM structure below $T_{N2} \sim 26$ K. Our ^{57}Fe Mössbauer spectroscopy indicates that there is the relative large IS and EQ hyperfine parameters of one sub-spectrum in the paramagnetic range. This is attributed to the presence of a *stable* Fe^{1+} , a seldom-observed state.

Acknowledgments: We would like to thank Gregory T. McCandless for drawing the structure of CaFe_4As_3 as shown in Figure 1. The research in Jerusalem is supported by the Israel Science Foundation (ISF, Bikura 459/09), and by the joint German-Israeli DIP. The work at LSU is supported by US NSF under grant No. DMR-1002622 (R. J.).

References

- Q. Huang, Y. Qiu, Wei Bao, M.A. Green, J.W. Lynn, Y.C. Gasparovic, T. Wu, G. Wu and [1]
X. H. Chen, Phys. Rev. Lett., **101**, 257003 (2008).

- [2] P. Zavalij, W. Bao, X. F. Wang, J. J. Ying, X. H. Chen, D. M. Wang, J. B. He, X. Q. Wang, G. F. Chen, P.-Y. Hsieh, Q. Huang, and M. A. Green, *Phys. Rev. B* **83**, 132509 (2011).
- [3] N. Ni, A. Thaler, J. Q. Yan, A. Kracher, E. Colombier, S. L. Bud'ko, and P. C. Canfield, *Phys. Rev. B* **82**, 024519 (2010).
- [4] A. P. Dioguardi, N. Roberts-Warren, A. C. Shockley, S. L. Bud'ko, N. Ni, P. C. Canfield, and N. J. Curro, *Phys. Rev. B* **82**, 140411(R) (2010).
- [5] R. H. Liu, X. G. Luo, M. Zhang, A. F. Wang, J. J. Ying, X. F. Wang, Y. J. Yan, Z. J. Xiang, P. Cheng, G. J. Ye, Z. Y. Li, and X. H. Chen, *Europhys. Lett.* **94**, 27008 (2011).
- [6] Z. Shermadini, A. Krzton-Maziopa, M. Bendele, R. Khasanov, H. Luetkens, K. Conder, E. Pomjakushina, S. Weyeneth, V. Pomjakushin, O. Bossen, and A. Amato, *Phys. Rev. Lett.* **106**, 117602 (2011).
- [7] I. S. Todorov, D.Y. Chung, C.D. Malliakas, Q. Li, T. Bakas, A. Douvalis, G. Trimarchi, K. Gray, J.F. Mitchel, A.R. Freeman and M.G. Kanatzidis, *J. Am. Chem. Soc.*, **131**, 5405 (2009).
- [8] P. Manuel, L.C. Chapon, I.S. Todorov, D.Y. Chung, J-P. Castellán, S. Rosenkranz, R. Osbron, P. Toledano and M.G. Kanatzidis, *Phys. Rev. B* **81**, 184402 (2010).
- [9] A. B. Karki, G. T. McCandless, S. Stadler, Y. M. Xiong, J. Li, J. Y. Chan, and R. Jin, *Phys. Rev. B* **84**, 054412 (2011).
- [10] L. Zhao, T. Yi, J.C. Fettinger, S.M. Kauzlarich and E. Morosan, *Phys. Rev. B* **80**, 020404 (2009).
- [11] M.S. Kim, Z.P. Yin, L.L. Zhao, E. Morosan, G. Kotliar and M.C. Aronson, arXiv.1106.0480
- [12] I. S. Todorov, D.Y. Chung, H. Claus, K. Gray, Q. Li, J. Schleuter, T. Bakas, A.P. Douvalis, M. Gutmann and M.G. Kanatzidis, *Chem. Mater.*, **22**, 4996 (2010).
- [13] S.M. Dubil, *J. Alloys and Compounds* **448**, 18 (2009).
- [14] A. Blachowski, K. Ruebenbauer, J. Zukrowski, K. Rogacki, Z. Bukowski and J. Karpinski, *Phys. Rev. B* **83**, 134410 (2011).
- [15] I. Nowik, I. Felner, N. Ni, S. L. Bud'ko and P. C. Canfield, *J. Phys. Cond. Matter.*, **22**, 355701 (2010).
- [16] I. Nowik, I. Felner, M. Zhang, A. F. Wang and X. H. Chen, *Supercond. Sci. Technol.* **24**, 095015 (2011).
- [17] K. Ruebenbauer, U. D. Wdowik, M. Kwater, and J. T. Kowalik, *Phys. Rev. B* **54**, 12880 (1996).
- [18] J. Chappert, R.B. Frankel and N.A. Blum, *Phys. Letters* **25A**, 149 (1967).
- [19] J.G. Mullen, *Phys. Rev.* **131**, 1415 (1963).